J. Manuf. Innov.
DOI: 10.22055/JOMI.2024.45746.1013 Jomi.scu.ac.ir

Journal of Manufacturing Innovations

Research Paper

Fabrication of Al5083-(CeO_2-TiO_2) hybrid surface composite via friction stir processing combined with plasma electrolytic oxidation

Kiana Esfandmaz [1], Khalil Ranjbar [2]*, Mehdi Khorasanian [3]

[1,2,3] Materials Science and Engineering Department, Faculty of Engineering, Shahid Chamran University of Ahvaz, Iran

Received; 2024-01-03; Accepted for publication: 2024-01-14

* Corresponding author: Khalil Ranjbar (k_ranjbar@scu.ac.ir)

Abstract

Using friction stir process (FSP) followed by plasma electrolytic oxidation (PEO), a surface composite consisting of Al5083 alloy as the base metal and TiO_2 and CeO_2 particles as reinforcements was produced. During the PEO process, the base metal was coated with an oxide layer containing the reinforcing particles in an electrolytic solution. FSP was then applied to the PEO-coated base metal. The effect of these nano-sized reinforcements either individually or in combined form on the microstructure, surface hardness, wear behavior, and corrosion resistance of the FSPed samples was studied and compared with the base alloy with no reinforcing particles. The FSP was performed with a rotational speed of 1400 rpm, using a cylindrical threaded hardened steel pin. Optical and scanning electron microscope examinations revealed that the reinforcing particles were uniformly distributed inside the nugget zone (NZ). The PEO and FSP processes resulted in distribution of reinforcing particles, microstructural modification, and considerable improvement in mechanical properties and

corrosion resistance of the base alloy. The results showed that the 15 minutes plasma electrolytic oxidation of CeO_2 particles, resulted in the most improvement in hardness, corrosion resistance and wear resistance compared to other processing conditions. The corrosion behavior of the samples was evaluated by potentiodynamic polarization tests in a standard 3.5 wt. % NaCl solution. The study was aimed to fabricate surface composites with improved wear behavior and corrosion resistance simultaneously.

Keywords: Plasma electrolytic oxidation, Friction stir processing, Surface composite, Al5083 alloy, CeO_2, TiO_2, Corrosion, wear

1. Introduction

Plasma electrolytic oxidation (PEO) is a novel surface treatment that produces thick and dense metal oxide coatings, especially on light metal surfaces, primarily to improve their corrosion and wear resistance [1]. PEO usually employs an aqueous electrolyte in which the oxide coatings are formed under the application of high electric voltages [2]. The process is also known as micro-arc oxidation (MAO), plasma chemical oxidation (PCO), or anodic oxidation by spark discharge. Despite the presence of residual porosities, it can develop suitable coating with the right choice of the electrolyte and the microarcing voltage [1]. Similar to the PEO process, Friction stir processing (FSP) is also a surface modification treatment which is actually based on friction stir welding (FSW), where a rotating tool with a specially designed pin and shoulder travels along the desired path above a metallic substrate [3]. Through frictional heating and severe plastic deformation, the rotating tool creates a significant change in the local microstructure, with three distinct zones: the heat-affected zone (HAZ), the thermomechanically affected zone (TMAZ), and the nugget zone (NZ). Grain refinement takes place most seriously in NZ, because of the dynamic recrystallization and severe plastic deformation. In addition, FSP can produce surface composites by incorporating reinforcing particles. The reinforcement particles are introduced in a groove or hole on the surface of the base metal. The rotating pin promotes the mixing of particles with the processed metallic substrate near its surface. Therefore, though FSP has been developed as a grain reinforcement technique, it is a very attractive process for fabricating surface composites, in particular for aluminum alloys. Al5083 is an Al-Mg alloy with excellent properties, including low density, high specific strength, good formability, and excellent corrosion resistance in seawater, and it is widely used in the automobile and transportation industries, as well as the aerospace and marine applications [3]. Creating coatings on the surface of metals improves the corrosion and

wear properties of the materials and increases their efficiency in their application fields. Thus, by producing an oxide layer through the PEO process and applying FSP on the PEO coated surface, two surface treatments are combined which expected to have a strong effect on the hardness, wear resistance, and corrosion properties of the base alloy. It is necessary to control the different processing parameters to achieve desired properties in every case. In the case of PEO, the oxidation duration is very important and affects the corrosion resistance of the coating. Laleh et al. [4] conducted corrosion tests on the coating that was sealed in a Ce bath for 10 min, and their results showed a superior corrosion resistance than the other coating times. Tjong et al. [5] used Ce and La coatings on Al composite substrate, and concluded that both cerium and lanthanum reduced the corrosion rate of the substrate. Ghasemi et al. [6] studied the effect of porous and compact layers of the PEO coating, and concluded that the overall coating resistance is mainly dependent upon the compactness of the layer. Bahramian et al. [7] examined the addition of TiO_2 nanoparticles into an electrolyte, and produced a dense coating on the surface of an Al alloy. The PEO composite coating exhibited superior corrosion behavior and mechanical properties compared to the PEO coating with no oxide particles. Similar results were reported by Sung et al. [8] with direct deposition of Ti-oxides on an Al metal surface by the PEO process. Modification of the surface properties including hardness, wear behavior and corrosion resistance have also been practiced through FSP. Zad Ali et al. [9] fabricated surface composites of Al3003 alloy reinforced with zirconium particles with different passes of FSP. They reported in-situ formation of Al_3Zr during FSP which contributed to a significant improvement of mechanical properties. Amra et al. [10], and Hosseini et al. [11] used FSP to develop surface composites of Al5083 alloy with CeO_2 + SiC, and CeO_2 + CNTs reinforcement particles, respectively. In both cases, the FSPed composites showed a considerable improvement in mechanical properties and corrosion resistance. Further modifications and enhancements of the surface properties by combining both PEO and FSP have been reported, as well. Chen et al. [12] used a silicate electrolyte and applied a ceramic coating by PEO process to an FSWed surface joint of AZ31B magnesium alloy. The PEO surface treatment significantly improved the corrosion resistance of the joint. A similar conclusion was reported by Srinivasan et al. [13] assessing the effect of PEO surface coatings on the corrosion behavior of the FSWed AZ61 alloy.

2. Materials and Methods

A sheet of Al5083 Aluminum alloy in annealed condition was used as the base alloy. Its chemical composition is given in **Table 1**. Rectangular samples (5 × 100 ×170 mm^3) were prepared for PEO and FSP.

Table 1 Chemical composition of the base alloy Al5083 used in the present study

Elements	Zn	Cu	Ti	Si	Cr	Fe	Mn	Mg	Al
wt. %	0.061	0.06	0.04	0.22	0.11	0.4	0.4	4.51	Bal.

The electrolyte bath used for PEO was an aqueous solution of sodium silicate (Na_2SiO_3), and starch. Various amounts of titanium oxide and cerium oxide particles were added to the electrolyte. First, the starch was dissolved in distilled water, and then the rest of the materials were added and mixed to form a homogenous solution. The coating process was performed by a plasma electrolytic oxidation apparatus (DC 6 kW 3-phase power supply). Each sample was processed in the electrolyte solution for 15 minutes during the PEO process under 175 V. Finally, an electrolyte solution with oxide particles (1 wt.% each) was prepared either individually or in combination.

One of the samples coated by PEO process is shown in **Fig. 1a**, and the schematic view of the combined PEO and FSP is shown in **Fig. 1b**. For the FSP, the rotating tool was made of H13 hot worked tool steel, which had been heat treated to a surface hardness of 52HRC. Cylindrical concave shoulder had the diameter of 18 mm and the threaded pin had the length and the diameter of 4.5 and 6 mm, respectively. Then, the pin is attached to the shoulder, plunged into the PEO coated plate, and travelled across the length of the plate. The PEO coated plate after applying three passes of FSP is shown in **Fig. 1c**. All passes were performed at a rotational speed of 1400 rpm and a traveling speed of 40 mm/min.

Microstructural observation was performed using optical microscope (∑GMA/VP-ZESIS) and field emission scanning electron microscope (FE-SEM: VEGA-TSCAN) equipped with an energy dispersive X-ray spectroscopy (EDS) system. Samples were cut from the cross section of the processed samples, polished by alumina suspension, and etched with modified Poulton's reagent solution (2.5 mL HF + 30 mL HCl + 40 mL HNO_3 + 42.5 mL distilled water and 12 g Cr_2O_3)[14].

The hardness profile along the cross section of the FSPed samples was also determined by a microhardness test using a Vickers indenter at the load of 200 g and dwell time of 10 s. The average hardness value is reported based on 3 measurements.

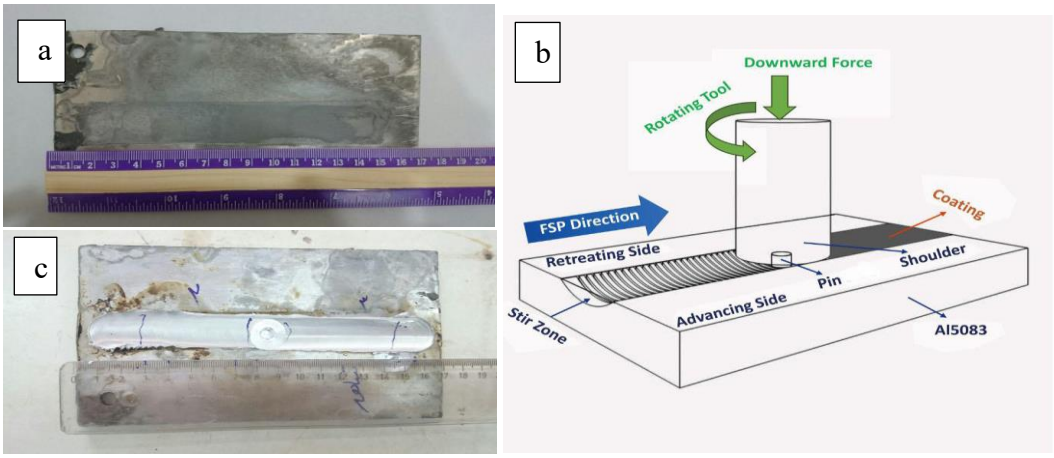

Fig. 1 a) A PEO coated sample before FSP, b) a schematic view of the combined PEO and FSP and, c) a PEOed plate after performing FSP

To conduct the potentiodynamic polarization tests, samples were cut from NZ and prepared according to the ASTM-G3 standard. All corrosion tests were conducted in a 3.5% NaCl solution prepared by dissolving 35 g of NaCl in double distilled water, at a scan rate of 0.5 mV/s using an AUTO LAB potentiostat–galvanostat model AUT8491. Temperature and the pH of the electrolyte were maintained at 25 °C and 7, respectively. An electrochemical cell consisting of platinum as an auxiliary electrode, saturated calomel electrode as a reference electrode (SCE), and the samples taken from NZ as a working electrode were used. All the experimental potential data presented in this paper are called according to this saturated calomel reference electrode. The potential scan used to determine the polarization curves was carried out in the range of -0.5 to 0.5 V/SCE. Before each polarization test, the sample was immersed in the test solution for 15 minutes at the open circuit potential (OCP), stabilizing the system. An exposure area of 25 mm^2 from SZ was subjected to the corrosion tests and the rest were covered with epoxy. At least three separate samples were tested for each group to ensure the reproducibility of the results.

The wear behavior of the FSPed samples was assessed using a pin-on-disk wear testing device at room temperature, against the counterface of a hardened disk of AISI 52100 steel with a hardness of HRC60. A cylindrical pin specimen with a diameter of 5 mm was machined from the NZ. The wear test was carried out at a load of 10 N at a speed of 100 rpm for 500 m. The

specimens were weighed before testing, and during testing, after every 100 m sliding, to determine the weight loss

3. Results and Discussion

3.1 Microstructure

An optical micrograph of the Al5083 base alloy before PEO and FSP is presented in **Fig. 2a**. As shown in the figure, grains are equiaxed with an average size of about 60 μm. The size of the grains decreased significantly after being subjected to FSP as shown in **Fig. 2b**. The latter case involves a clear modification and refinement of grain structure, where the grain size changes to a more homogeneous, equiaxed, and smaller one. This is attributed to the severe plastic deformation, mechanical mixing, and frictional heat generated during FSP which causes dynamic recrystallization and leads to grain refinement [3]. When severe plastic deformation occurs in the NZ, the flow stress rises where dislocations multiply, interact, and re-arrange to form low-angle boundaries, which are ideal for nucleating new crystals [15]. The process of dynamic recrystallization transforms low-angle disoriented grain boundaries into high-angle disoriented grain boundaries, which results in fine equiaxed grains [16], [17]. Additionally, particle-simulated nucleation (PSN) occurs in the Al5083 alloy due to intermetallic particles [18], [19]. **Fig. 3** shows the scanning electron micrographs of the PEO coating created within 15 minutes. According to the figure, the thickness of the coating is less than 1 μm. The coating is composed of a ceramic oxide layer (Al_2O_3), which is brittle and porous, with microcracks. These coatings often peel off and separate from sample surfaces due to excessive brittleness [11].

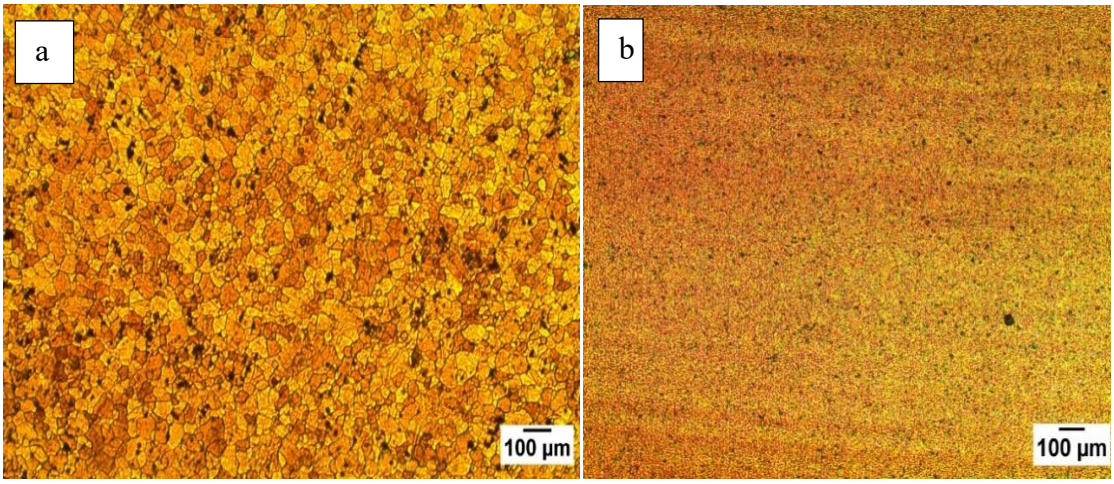

Fig. 2 Optical micrographs of the base alloy Al5083, a) before FSP, and b) after FSP with reinforcement

Fig. 4 shows the different FSPed regions after three FSP passes. Different distinct regions of NZ, TMAZ, and onion rings are shown. Performing three passes of FSP eliminates onion rings, refines grains, and modifies the size and distribution of the intermetallics. The process of refinement and modification is most prevalent in SZ, and to a lesser extent in TMAZ. Plastic deformation and frictional heating are not sufficient to promote dynamic recrystallization in the latter case, so TMAZ is partially modified. **Fig. 5** shows a sample in which both titanium oxide and cerium oxide particles were added to the plasma oxidation solution, and after three passes of FSP, uniform distribution of the particles was achieved. Analysis of cerium oxide particles is presented in **Table 2**. These reinforcing particles also act as a grain growth inhibitor causing further grain refinement.

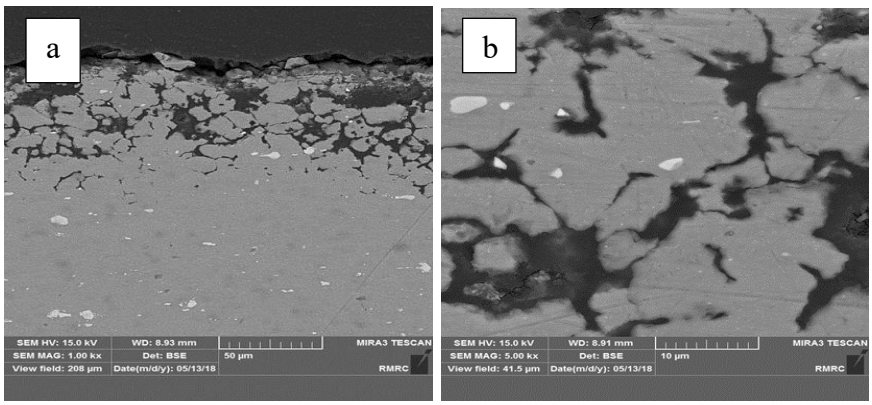

Fig. 3 SEM images showing PEO coating produced in electrolyte containing 20 g/l sodium silicate, 4 g/l titanium oxide, 300 g/l starch, with a coating time of 15 minutes

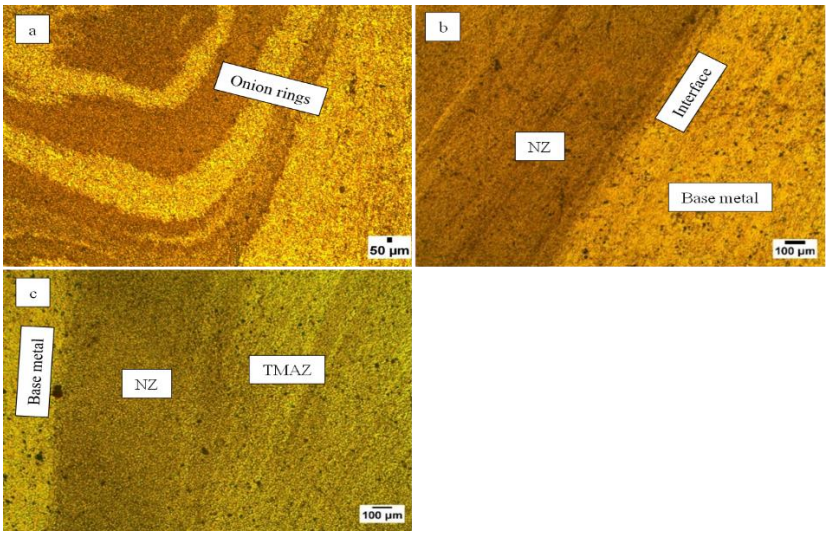

Fig. 4 Microstructural features of Al5083 after subjecting PEO and then FSP with CeO2 reinforcing particles, a) appearance of opinion rings after two passes, b) interface between NZ and the base metal with no apparent defects, and, c) different zones of base metal, NZ, and TMAZ

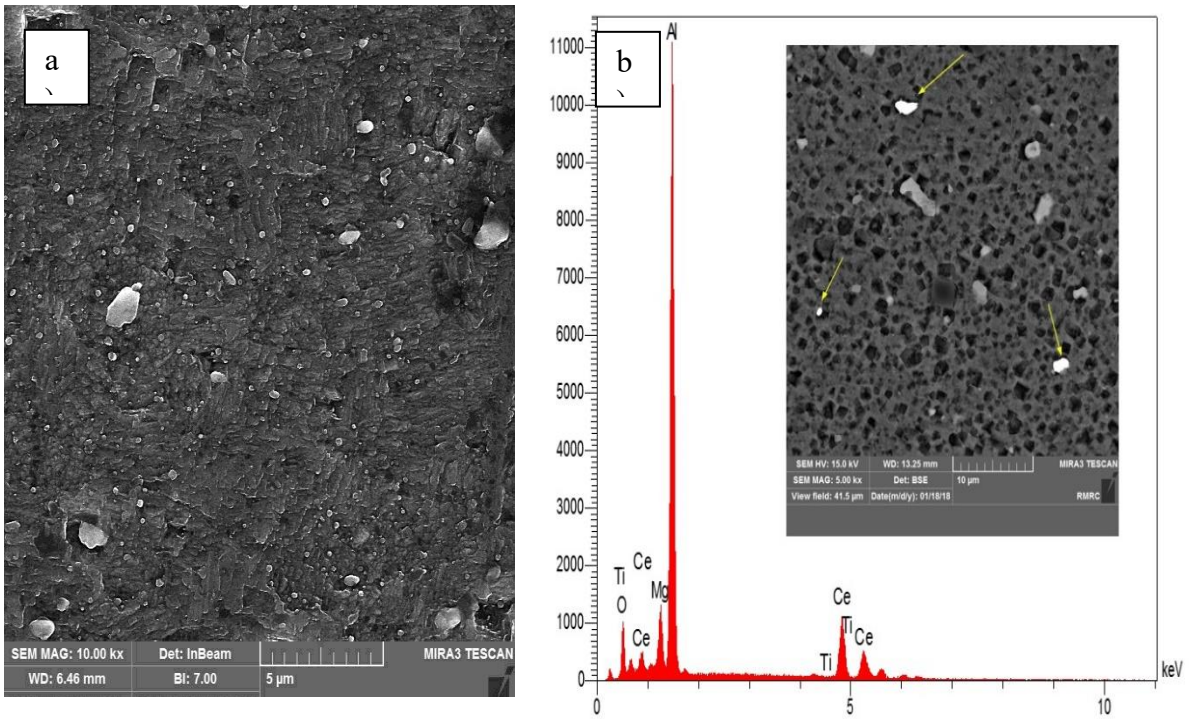

Table 2 Composition of the points marked by arrows and analyzed by EDS

Element	O	Mg	Al	Ce
Wt.%	11.72	4.87	46.81	36.60

Fig. 5 a) FESEM image of Al5083/CeO_2/TiO_2 nanocomposite shows the distribution of CeO_2 and TiO_2 particles in the nanocomposite matrix, and b) SEM image and EDS chemical analysis of points marked by the arrows. The corresponding composition is given in the Table 2

3.2 Corrosion behavior

To assess the corrosion behavior of the base alloy as well as FSPed samples, potentiodynamic polarization tests were carried out. The results are presented by potentiodynamic polarization curves in **Fig. 6**. The corrosion potential (E_{corr}) and the corrosion current density (i_{corr}) derived from these curves (Tofel extrapolation) are also shown in **Table 3**. Aluminum and its alloys are corrosion resistant because of the tightly bonded oxide film formed on their surface in contact with air and water. This oxide film may fail when it is exposed to salt water or alkaline solutions, since the film may dissolve and result in localized corrosion. The formation of such a protective layer is called passivity and is defined as a reduction in the chemical or electrochemical activity of the metal interacting with the environment [14]. To investigate the effect of the coating on the corrosion resistance, the potentiodynamic polarization test was performed in a solution of 3.5 wt.% sodium chloride at room temperature (25°C). As shown in

Table 3, the sample that contains cerium oxide particles has a current density of 1.17 μA/cm^2, which has a lower current and better corrosion resistance than all of the samples. The results of adding CeO_2 show its performance as a corrosion inhibitor and a significant reduction in the corrosion current density can be observed. The mechanisms of improving the corrosion properties by addition of CeO_2 include encouraging the growth of the protective oxide layer, improving the cohesion, and strengthening the oxide layer [20]–[22]. Similarly, with incorporation of TiO_2 nanoparticles, the matrix grains were refined and the coating became more compact. Therefore, corrosion currents distribute more evenly and, as a result, the corrosion resistance is improved.

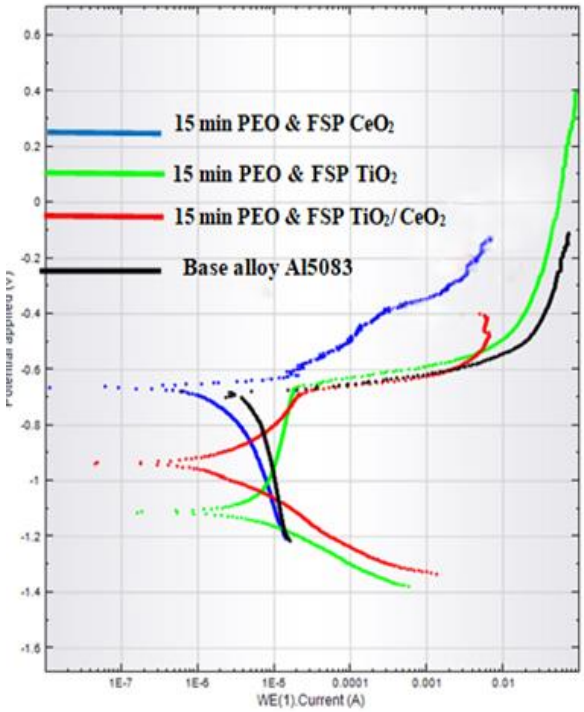

Fig. 6 Potentiodynamic polarization curves of the base alloy and specimens subjected to PEO process for 15 minutes and then FSP

Table 3 The summary of potentiodynamic polarization test results conducted in a 3.5% NaCl solution at room temperature after 15 min. of PEO and the subsequent FSP

Samples	E_{corr} (mv)	i_{corr} (μA/cm^2)
Base alloy Al5083	-678	14.3
PEO & FSP TiO_2	-1111	3.2
PEO & FSP CeO_2	-658	1.17
PEO & FSP TiO_2/CeO_2	-930	2.89

3.3 Microhardness

Fig.7 shows the microhardness profiles of samples that were processed using a combination of PEO and FSP. The hardness of the processed alloy is higher than the unprocessed base metal due to friction stirring. The sample containing cerium oxide demonstrated the maximum hardness, followed by the sample containing titanium oxide. The oxide reinforcing particles are evenly distributed within the processed zone during the stirring process. This is accompanied by severe plastic deformation and dynamic recrystallization, leading to grain refinement and preventing plastic deformation by inhibiting dislocation movement. According to the Hall-Petch equation, finer grains are associated with greater strength and hardness values. The highest hardness values for all the FSPed samples were found in the NZ.

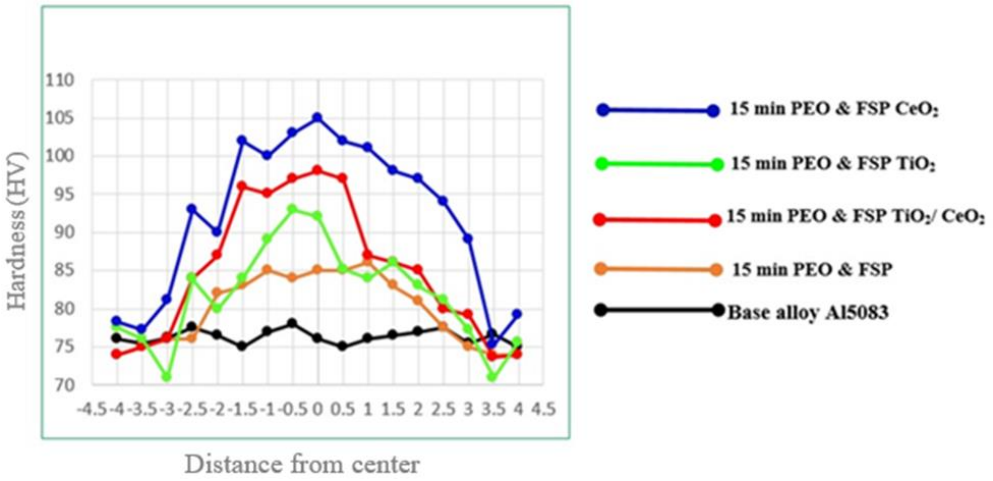

Fig. 7 The microhardness profiles of the base alloy and the composite samples that underwent combined PEO and FSP.

3.4 Wear behavior

Fig. 8 shows that the weight loss of all samples increased with sliding distance during the wear test. Weight loss, which measures the wear damage, follows the same trend of the hardness values presented in **Fig. 7**. It is evident that the wear resistance of samples treated with PEO and FSP, individually or combined, improved compared to untreated samples. The sample with cerium oxide exhibited the lowest weight loss due to the high hardness of the nanoparticles, as well as grain refinement resulting from dynamic recrystallization. The base metal showed the highest weight loss value.

SEM micrographs of the worn surfaces under identical conditions are shown in **Fig. 9**. The samples were first treated with PEO and reinforcing particles, followed by FSP. The untreated metal exhibited plastic deformation and deep grooves (**Fig. 9a**) due to its large grain size and

low hardness. In this sample, wear debris were in the form of large wear flakes (**Fig. 9b**). The combined effect of reinforcing particles was noticeably different, as shown in **Fig. 9c** and **Fig. 9d**. In this case, the wear mechanism was adhesive wear, unlike the abrasive wear mechanism noticed in samples containing individual oxide particles shown in **Fig. 9e** and **Fig. 9f**. Therefore, based on the results in **Fig. 8** and **Fig. 9**, the wear mechanism was adhesive in hybrid samples and abrasive in individual oxide-reinforced samples.

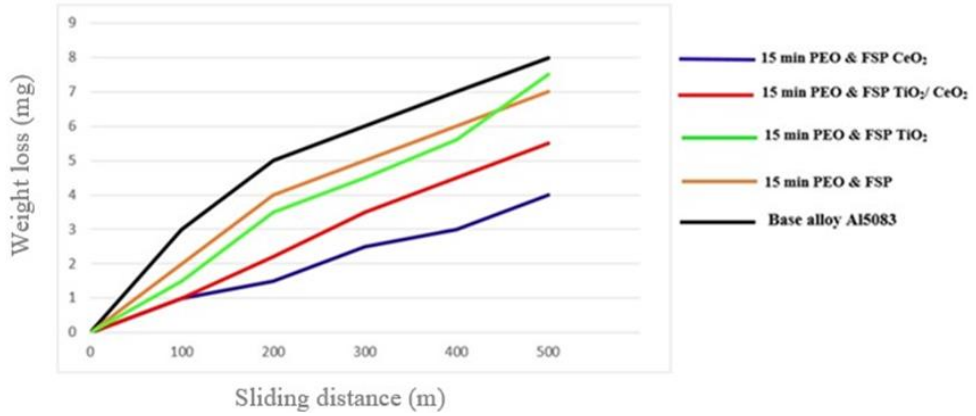

Fig. 8 Variation of weight loss with the sliding distance for different processed samples

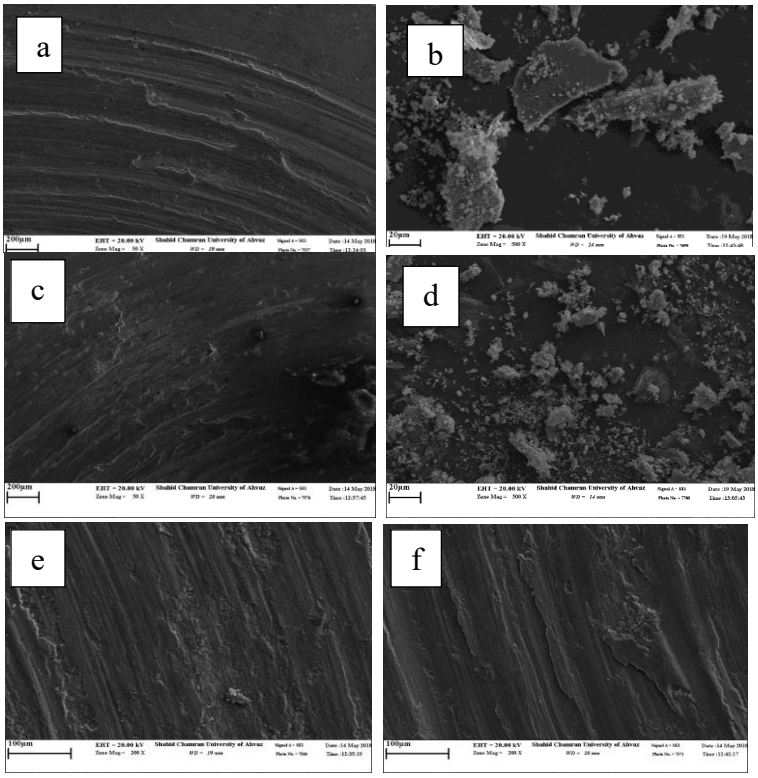

Fig. 9 Wear surface morphologies after testing for different samples processed initially by the PEO and then subjected to FSP: a) base metal (unprocessed), b) wear debris for the base metal, c) sample

with both TiO_2+CeO_2 particles, d) wear debris for sample shown in c. Wear track for the samples with individual TiO_2 and CeO_2 particles, respectively

4. Conclusions

Surface composites of Al5083 were produced in this research using a combination of plasma electrolytic oxidation and friction stir process methods. TiO_2 and CeO_2 particles were used as reinforcements. The process involved adding reinforcing particles to the electrolytic solution, which was then PEOed, and subjected to three passes of FSP.

The microstructural investigations showed that the reinforcing particles were evenly distributed in the stir zone. Samples with reinforcing particles underwent significant grain refinement compared to the base alloys. They exhibited higher hardness values and wear resistance. The Al5083-CeO_2 sample showed the maximum hardness, wear resistance, and corrosion resistance. Wear mechanism was adhesive in hybrid samples and abrasive in individual oxide reinforced samples. Based on the results, it can be concluded that PEO and FSP can be successfully combined to improve the surface hardness and wear properties of the Al5083 alloy.

References

[1] G. Zhao and J. Zhao, “Surface modification of die casting mold steel by a composite technique of hot-dipping and plasma electrolytic oxidation,” *Rare Met.*, vol. 31, no. 4, pp. 362–367, Aug. 2012, doi: 10.1007/s12598-012-0521-8.

[2] J. A. Curran and T. W. Clyne, “Thermo-physical properties of plasma electrolytic oxide coatings on aluminium,” *Surf. Coatings Technol.*, vol. 199, no. 2–3, pp. 168–176, Sep. 2005, doi: 10.1016/j.surfcoat.2004.09.037.

[3] R. S. Mishra and Z. Y. Ma, “Friction stir welding and processing,” *Mater. Sci. Eng. R Reports*, vol. 50, no. 1–2, pp. 1–78, Aug. 2005, doi: 10.1016/j.mser.2005.07.001.

[4] M. Laleh, F. Kargar, and A. S. Rouhaghdam, “Investigation of rare earth sealing of porous micro-arc oxidation coating formed on AZ91D magnesium alloy,” *J. Rare Earths*, vol. 30, no. 12, pp. 1293–1297, Dec. 2012, doi: 10.1016/S1002-0721(12)60223-3.

[5] S. C. Tjong and H. W. Huo, “Corrosion Protection of In Situ Al-Based Composite by Cerium Conversion Treatment,” *J. Mater. Eng. Perform.*, vol. 18, no. 1, pp. 88–94, Feb. 2009, doi: 10.1007/s11665-008-9264-y.

[6] A. Ghasemi, V. S. Raja, C. Blawert, W. Dietzel, and K. U. Kainer, “Study of the

structure and corrosion behavior of PEO coatings on AM50 magnesium alloy by electrochemical impedance spectroscopy," *Surf. Coatings Technol.*, vol. 202, no. 15, pp. 3513–3518, Apr. 2008, doi: 10.1016/j.surfcoat.2007.12.033.

[7] A. Bahramian, K. Raeissi, and A. Hakimizad, "An investigation of the characteristics of Al2O3/TiO2 PEO nanocomposite coating," *Appl. Surf. Sci.*, vol. 351, pp. 13–26, Oct. 2015, doi: 10.1016/j.apsusc.2015.05.107.

[8] D. Sung, D. Kim, J.-H. Park, Y. Kim, and W. Chung, "Effect of composite PEO film containing titanium oxides on the corrosion resistance of Al 6061 alloy," *Surf. Coatings Technol.*, vol. 309, pp. 698–702, Jan. 2017, doi: 10.1016/j.surfcoat.2016.11.005.

[9] M. Z. M. Kotiyani, K. Ranjbar, and R. Dehmolaei, "In-situ fabrication of Al 3 Zr aluminide reinforced AA3003 alloy composite by friction stir processing," *Mater. Charact.*, vol. 131, pp. 78–90, Sep. 2017, doi: 10.1016/j.matchar.2017.06.028.

[10] M. AMRA, K. RANJBAR, and S. A. HOSSEINI, "Microstructure and wear performance of Al5083/CeO2/SiC mono and hybrid surface composites fabricated by friction stir processing," *Trans. Nonferrous Met. Soc. China*, vol. 28, no. 5, pp. 866–878, May 2018, doi: 10.1016/S1003-6326(18)64720-X.

[11] S. A. Hosseini, K. Ranjbar, R. Dehmolaei, and A. R. Amirani, "Fabrication of Al5083 surface composites reinforced by CNTs and cerium oxide nano particles via friction stir processing," *J. Alloys Compd.*, vol. 622, pp. 725–733, Feb. 2015, doi: 10.1016/j.jallcom.2014.10.158.

[12] G.-H. Lv *et al.*, "Effect of additives on structure and corrosion resistance of plasma electrolytic oxidation coatings on AZ91D magnesium alloy in phosphate based electrolyte," *Surf. Coatings Technol.*, vol. 205, pp. S36–S40, Dec. 2010, doi: 10.1016/j.surfcoat.2010.03.035.

[13] P. Bala Srinivasan, R. Zettler, C. Blawert, and W. Dietzel, "A study on the effect of plasma electrolytic oxidation on the stress corrosion cracking behaviour of a wrought AZ61 magnesium alloy and its friction stir weldment," *Mater. Charact.*, vol. 60, no. 5, pp. 389–396, May 2009, doi: 10.1016/j.matchar.2008.10.010.

[14] M. Amra, K. Ranjbar, and R. Dehmolaei, "Mechanical Properties and Corrosion Behavior of CeO2 and SiC Incorporated Al5083 Alloy Surface Composites," *J. Mater.*

Eng. Perform., vol. 24, no. 8, pp. 3169–3179, Aug. 2015, doi: 10.1007/s11665-015-1596-9.

[15] F. J. Humphreys, P. B. Prangnell, and R. Priestner, "Fine-grained alloys by thermomechanical processing," *Curr. Opin. Solid State Mater. Sci.*, vol. 5, no. 1, pp. 15–21, Jan. 2001, doi: 10.1016/S1359-0286(00)00020-6.

[16] A. H. Feng and Z. Y. Ma, "Microstructural evolution of cast Mg–Al–Zn during friction stir processing and subsequent aging," *Acta Mater.*, vol. 57, no. 14, pp. 4248–4260, Aug. 2009, doi: 10.1016/j.actamat.2009.05.022.

[17] D. Yadav and R. Bauri, "Nickel particle embedded aluminium matrix composite with high ductility," *Mater. Lett.*, vol. 64, no. 6, pp. 664–667, Mar. 2010, doi: 10.1016/j.matlet.2009.12.030.

[18] M. A. García-Bernal, R. S. Mishra, R. Verma, and D. Hernández-Silva, "Hot deformation behavior of friction-stir processed strip-cast 5083 aluminum alloys with different Mn contents," *Mater. Sci. Eng. A*, vol. 534, pp. 186–192, Feb. 2012, doi: 10.1016/j.msea.2011.11.057.

[19] L. B. Johannes, I. Charit, R. S. Mishra, and R. Verma, "Enhanced superplasticity through friction stir processing in continuous cast AA5083 aluminum," *Mater. Sci. Eng. A*, vol. 464, no. 1–2, pp. 351–357, Aug. 2007, doi: 10.1016/j.msea.2007.02.012.

[20] S. Di, Y. Guo, H. Lv, J. Yu, and Z. Li, "Microstructure and properties of rare earth CeO2-doped TiO2 nanostructured composite coatings through micro-arc oxidation," *Ceram. Int.*, vol. 41, no. 5, pp. 6178–6186, Jun. 2015, doi: 10.1016/j.ceramint.2014.12.134.

[21] A. Ghasemi-Kahrizsangi and S. F. Kashani-Bozorg, "Microstructure and mechanical properties of steel/TiC nano-composite surface layer produced by friction stir processing," *Surf. Coatings Technol.*, vol. 209, pp. 15–22, Sep. 2012, doi: 10.1016/j.surfcoat.2012.08.005.

[22] T. N. Rhys-Jones, H. J. Grabke, and H. Kudielka, "The effects of various amounts of alloyed cerium and cerium oxide on the high temperature oxidation of Fe-10Cr and Fe-20Cr alloys," *Corros. Sci.*, vol. 27, no. 1, pp. 49–73, Jan. 1987, doi: 10.1016/0010-938X(87)90119-3.